

Density Adapted Stack of Stars Sequence for ^{23}Na Imaging at 7T

Fabian J Kratzer¹, Sebastian Flassbeck¹, Simon Schmidt¹, Armin M Nagel^{1,2}, Peter Bachert¹, Mark E Ladd¹, Nicolas G R Behl¹

¹Medical Physics in Radiology, German Cancer Research Center (DKFZ), Heidelberg, Germany; ²Institute of Radiology, University Hospital Erlangen, Erlangen, Germany

Target audience: Physicists and clinicians interested in ^{23}Na MRI

Purpose/Introduction: Due to its quadrupole moment, ^{23}Na MRI suffers from short relaxation times¹. Hence it is beneficial to use dedicated k-space sampling schemes, such as radial or spiral trajectories to obtain short echo times. Conventional radial sampling results in a decreasing sampling density, when going towards higher k-space frequencies. The use of density adapted gradients, consisting of a trapezoidal and a density adapted part, ensures more homogenous sampling density. This results in an increased SNR and less artifacts, as previously shown^{2,3}. However, the measurement times for 3D radial acquisition can be long, especially if only a limited number of slices are of interest. Hence a 2D density adapted radial sequence was previously presented³. This leads to a theoretical SNR gain of up to 15.5% compared to standard radial imaging³. Fast transverse relaxation can further increase the SNR gain (in particular if small structures are analyzed). For more flexibility, we present a density-adapted stack of stars (DA-SOS) sequence, where the same SNR gain holds. This enables 3D imaging with a varying field of view (FOV) in z-direction and the optimization of scanning time for a given structure. Furthermore, it allows anisotropic imaging which can be exploited in structures that display limited variation in a certain direction, e.g. muscle tissue.

Methods: Due to hardware limitations the readout gradient starts with a trapezoidal gradient, with amplitude G_0 , at the end of which the k-space position $k_0 = k(t_0)$ is reached. The subsequent density adapted section can be written as³: $G(t) = \frac{k_0 G_0}{\sqrt{k_0^2 + 2\gamma k_0 G_0 (t - t_0)}}$. Cartesian sampling is used in z-direction. A sequence diagram is shown in Fig. 1. Either a spoiler gradient or a rewinder can be used following the readout gradient. For comparison, the sequence provides the possibility of conventional and density adapted (DA) readout gradients. Furthermore each star can be acquired with fixed angle increment, as well as a golden angle sampling (including tiny golden angles⁴, $N=1\dots 10$).

The reconstruction was implemented in MATLAB (Mathworks, Natick, USA) using a non-uniform Fast Fourier Transform (nuFFT)⁵. Furthermore, the sequence was evaluated using simulations⁶, Gaussian noise was added to match the SNR of the measurements. Measurements were performed on a 7T whole body scanner (Magnetom 7T, Siemens, Erlangen, Germany) with a $^1\text{H}/^{23}\text{Na}$ double resonant birdcage coil (Rapid Biomed GmbH, Rimpar, Germany), where the proton channel was used for B_0 shimming. For proof of concept, in vivo measurements were performed on a healthy volunteer (24, male, 95 kg).

Results: The SNR in white matter (WM) and cerebrospinal fluid (CSF) was calculated with a ROI evaluation.

Resulting images are shown in Fig. 2 (1 slab, 8 partitions, $3 \times 3 \times 5 \text{ mm}^3$, TE/TR = 1.01/39.5 ms, nominal FA = 40° , 6 averages, 9:29 min). Using the density adapted sampling scheme the SNR was increased by 16.8% up to 49.6%, whereas the SNR gain for simulations was 6.3% to 20.4% (see Tab. 1).

Discussion & Conclusion: In this work a density adapted stack of stars sequence was presented, and it was shown that the SNR is increased when compared to trapezoidal readout. The sequence is applicable for ^{23}Na imaging of structures covering only a few slices, as well as for anisotropic imaging. For further increasing the SNR the echo time could be shortened via asymmetric pulses.

References: 1. Konstandin et al., MAGMA. 2014 27: 1-4; 2. Nagel et al., Magn Reson Med. 2009 62: 1565-1573; 3. Konstandin et al., Magn Reson Med 2011 65(4):1090-1096; 4. Wundrak et al., Magn Reson Med. 2016 75(6): 2372-2378; 5. Fessler et al., IEEE T-SP. 2003 51(2):560-574; 6. Lommen et al., Proc. ISMRM 2017: 5628

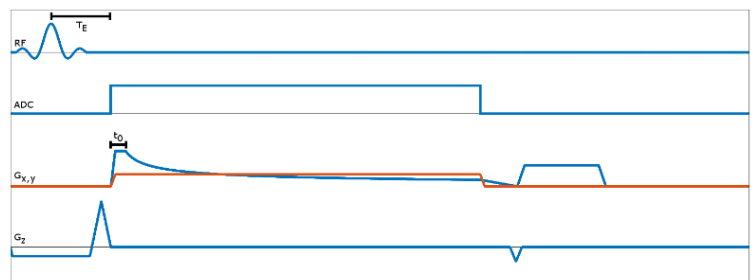


Figure 1: Sequence diagram of a spoiled 3D density-adapted (blue $G_{x,y}$) and a conventional (red $G_{x,y}$) stack of stars sequence.

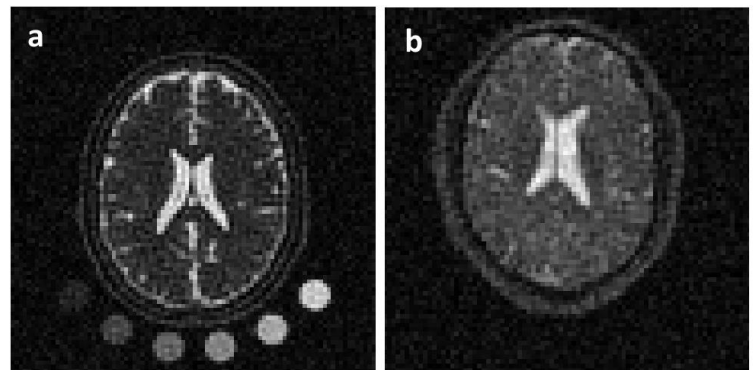


Figure 2: (a) Unfiltered simulation results of a density adapted stack of stars sequence and (b) the central partition of the corresponding 3D in vivo measurement (1 slab, 8 partitions, $3 \times 3 \times 5 \text{ mm}^3$, TE/TR = 1.01/39.5 ms, FA = 40° , 6 averages, 9:29 min).

Resolution, ROI	SNR DA	SNR not DA	Relative SNR (%)	Relative SNR simulated (%)
$3 \times 3 \times 5 \text{ mm}^3$, CSF	19.6	16.2	121.0	106.3
$3 \times 3 \times 5 \text{ mm}^3$, WM	6.3	4.2	149.6	120.4
$1.5 \times 1.5 \times 5 \text{ mm}^3$, CSF	7.4	6.1	120.8	117.4
$1.5 \times 1.5 \times 5 \text{ mm}^3$, WM	2.3	2.0	116.8	110.3

Table 1: Comparison of measured (1 slab, 8 partitions, $3 \times 3 \times 5 \text{ mm}^3 / 1.5 \times 1.5 \times 5 \text{ mm}^3$, TE/TR = 1.01/39.5 ms, FA = 40° , 6 averages, 300/600 spokes, 9:29/18:58 mins) and simulated SNR improvement due to density adaption.